MEASUREMENTS OF OPTICAL ATMOSPHERIC QUANTITIES IN EUROPE AND THEIR APPLICATION TO MODELLING VISIBLE SPECTRUM CONTRAST TRANSMITTANCE

Richard W. Johnson and Wayne S. Hering
University of California, San Diego
Scripps Institution of Oceanography
Visibility Laboratory

ABSTRACT

An 80 flight series of simultaneous optical and meteorological measurements between ground level and an altitude of 6 km has been gathered by the Visibility Laboratory under the sponsorship of the Air Force Geophysics Laboratory. These flights were conducted as an independent but related adjunct to the NATO Program OPAQUE. Data flights were conducted over several European sites during each of five separate two month periods selected to be representative of each of the four temporal seasons.

Illustrative data representing altitude profiles of visible spectrum scattering characteristics are presented, as are the simultaneous measurements of ambient and dewpoint temperatures. In addition to these profile data, several contemporaneous sets of multi-spectral directional volume scattering function measurements at scattering angles of 30 and 150 degrees are presented. The use of these data as a basis for the development of a technique for estimating atmospheric path radiance and contrast transmittance is discussed.

A computer model for the estimation of these atmospheric properties that is relatively fast and easy to apply is described with examples of its performance. The model input parameters are wavelength, extra-terrestrial solar irradiance, solar zenith angle, the number of atmospheric layers selected and their altitude limits, the average optical scattering ratio and the single scattering albedo for each layer, and the terrain reflectance. Using a modelling approximation that relates the directional distribution of single scattering to the total volume extinction coefficient, and using the delta-Eddington method for calculating the diffuse radiative fluxes, the model predicts the directional path radiance and contrast transmittance of any slant atmospheric path as a function of wavelength.

1. INTRODUCTION

In the increasingly sophisticated world of electro-optical detection, search, and guidance, the requirement for establishing and predicting atmospheric influences on system performance continues to be a primary operational necessity. It is in this general context that the techniques discussed in this paper can most usefully be addressed. Thus, though the instrument development and data collection portions of this experimental program have been complete for some time, the analysis of the data is continuing, and the application of these analytic results is both timely and specifically germane to the problems of E/O performance within the lower troposphere.

The Visibility Laboratory has for a good number of years conducted an airborne measurement program in cooperation with, and under the sponsorship of the United States Air Force Geophysics Laboratory. For the past several years the program has been conducted as an independent but cooperative effort, Johnson, et al. (1979), in conjunction with the NATO program OPAQUE (Optical Atmospheric Quantities in Europe), Fenn (1978).

In the remainder of this note we will discuss briefly the measurement program, its resulting data base, and in more detail, the application of these data to the task of modelling tropospheric visible spectrum contrast transmittance.

2. AIRBORNE INSTRUMENTATION

The nephelometer system, designed and built at the Visibility Laboratory, Duntley, et al. (1977) provides measurements of both the total and directional volume scattering properties of its captured aerosol in four discrete spectral bands, as illustrated in Fig. 1. The measurements of total volume scattering coefficient are produced by optical integration over all scattering angles between 5° and 172° which are then corrected for potential truncation losses via the systems simultaneous directional scattering measurements. The measurements of directional volume scattering function are made at scattering angles of 30° (i.e. forward scatter) and 150° (i.e. backscatter). These narrow angle directional measurements provide the forward to backscattering ratios which

Upper and lower hemisphere scanning radiometers were designed for the measurement of sky and terrain radiance distributions. They operate in the same spectral bands as the nephelometer system, and provide 4π radiance maps processed to yield an average (5^{o} field of view) radiance value for each 6^{o} in azimuth and each 5^{o} in zenith angle. These automatic scanner systems were initially described in Duntley, et al. (1970) and since were equipped with remotely controlled neutral density filters to enhance their near sun measurement capabilities.

3. AIRBORNE MEASUREMENTS

Although there were nearly ninety data missions flown by the instrumented C-130 during the OPAQUE episode, as illustrated in Fig. 2 and Table 1, the general thrust of these data must be considered in the case study context rather than in the broader climatological context associated with the host nation's far more extensive set of surface measurements. Johnson, et al. (1979). Nonetheless, there are sufficient airborne measurements to clearly establish the essential aerosol scattering characteristics required for modelling those tropospheric optical properties most influencing slant path contrast transmittances. Selected samples of these data which have been used as validation data throughout the model development process are illustrated in Figs. 3 through 7 and discussed briefly in the following paragraphs.

3.1. Meteorological Properties

Measurements of atmospheric pressure, temperature and dewpoint temperature were made throughout each data mission in both the fixed altitude and ascent/descent flight modes. These data are illustrated in Figs. 3 and 4 which have been reproduced from Johnson and Gordon (1980). In each of these plots, the data represent four separate ascents or descents. Each profile is coded with a symbol that links it with its simultaneous optical data set. (see Fig. 1). There is good temporal stability within the temperature regime during the data interval as is indicated by the generally good reproducibility among the four separate profiles shown in Fig. 3. Additionally, and as will become apparent more importantly, one can see from the overlayed 1200z RAOB data that the vertical structure of the temperature profiles can be readily identified from either the fine structured aircraft data, or the more coarsely defined RAOB data.

In Fig. 4, relative humidity, as computed from the measured values of ambient and dewpoint temperature, has been plotted in the same format as used to display the temperature data. Whereas these derived values exhibit a significantly higher degree of temporal variability, the general reproduction of major structural characteristics, i.e. layers and trends, is maintained. It is immediately apparent however, from an examination of the RAOB data in Fig. 4, that major structural artifacts in derived properties can be missed if one uses measurements reported at inappropriate altitude increments. For example, note the strong moist layer in the Soesterberg data which is completely undetected in the RAOB profile. An immediate recommendation then for enhancing the utility of this type data for model development and/or tactical decision input would be to provide the basic RAOB data at standardized and relatively fine altitude increments similar to those inherent in aircraft soundings.

3.2. Optical Properties

The variation in scattering coefficient as a function of altitude is one of the essential requirements for accurate computations of slant path tropospheric contrast transmittance, and thus must be reliably modelled if one presumes to develop predictive capabilities. Profile measurements such as those illustrated in Fig. 5 can provide the data base required for this model development within the visible spectrum, and conceivably provide the necessary insights for extrapolation to longer optical wavelengths. The profile characteristics requiring specific attention are the number and depth of well defined and reasonably well mixed aerosol layers, the most representative value of scattering coefficient within each layer, and the directional scattering properties of the aerosol within each layer. The data in Fig. 5 identify the first two characteristics. In each case there are two well defined layers with the boundary at about 1200-1500 meters. The average value of scattering coefficient within each layer can be readily established subsequent to upper altitude stray light corrections based upon directional scattering and sky radiance measurements.

There is strong evidence that the specification of the directional scattering properties within each aerosol layer can be reasonably deduced from a knowledge of the total volume scattering coefficient alone. Johnson, et al. (1979) and Johnson (1981). An example of the data supporting this contention is illustrated in Fig. 6 from Johnson and Gordon (1980). In these data, directional scattering function measurements made by the Visibility Laboratory ground based nephelometer system are compared with similar data from Barteneva (1960). Whereas the Barteneva data represent over 600 sets of directional scattering measurements using photopic spectral response, the Visibility Laboratory data

represent measurements made in all four of the responses defined in Fig. 1.

The data shown in Fig. 6 have been normalized to reflect only aerosol scattering characteristics by using a ratio display format. Thus the vertical axis, Volume Scattering Function Ratio, represents the ratio of the volume scattering function $\sigma(z,\beta)$ to the Rayleigh (i.e. molecular) volume scattering function ${}_R\sigma(z,\beta)$ at the same scattering angle β. i.e. $\mathcal{Q}(z) = \sigma(z,\beta)/{}_R\sigma(z,\beta)$ where z is the altitude parameter. Likewise, the horizontal axis, Optical Scattering Ratio, represents the ratio of the total volume scattering coefficient s(z)) to the Rayleigh volume scattering coefficient ${}_Rs(z)$. i.e. $Q(z) = s(z)/{}_Rs(z)$. These data and their airborne equivalents specifically support the contention that one can develop a parameterization that will adequately represent the directional scattering properties of an atmospheric aerosol once the optical scattering ratio Q(z) is specified, a fundamental simplification in any modelling attempt.

Our second major data set appropriate to the determination of tropospheric slant path contrast transmittances contains simultaneous measurements of sky and terrain radiances as determined from each of several different flight altitudes. In Fig. 7, the apparent radiances throughout the combined upper and lower hemispheres which surrounded the aircraft during flight C-466 are defined in one graph. Each of the four individually coded plots represents the observed radiance along a vertical sweep from the zenith through the horizon to the nadir and is at a fixed and constant azimuth from the sun.

The multi-spectral data typified by those illustrated in Fig. 7 provide a complete magnitude specification of the directional radiance field surrounding the aircraft. Thus they represent the net effects of the solar irradiance upon the total atmosphere within which the aircraft is implanted, including the influence of the underlying terrain. It is these data then, that allow one to close the modelling loop, in that they represent an essential intermediate step that a model must duplicate if it is to proceed to the subsequent determination of slant path contrast transmittance.

4. EXPRESSIONS FOR PATH RADIANCE AND CONTRAST TRANSMITTANCE

The analytic expressions relating the fundamental equation of radiative transfer to the apparent spectral radiance of a distant target, and the apparent contrast of that target as observed against its background are well developed by Duntley, et al. (1957). Those most directly related to the development of the modelling concepts discussed herein are summarized below.

The apparent spectral radiance of a target t at a range r, as measured from an altitude z in a direction defined by zenith angle θ and azimuth angle ϕ is

$$ {}_tL_r(z,\theta,\phi) = T_r(z,\theta,\phi){}_tL_o(z_t,\theta,\phi) + L_r^*(z,\theta,\phi) \tag{1} $$

where ${}_tL_o$ is the inherent spectral radiance of the target, T_r is the spectral transmittance of the path, and L_r^* is the directional path radiance.

As discussed in Duntley, et al. (1957), the directional path radiance is derived from the integration along the path of sight of the directional path function $L_\bullet(z,\theta,\phi)$ which is defined as the point function component of path radiance generated by the scattering of light reaching that point from all points within its surrounding field.

The expression for the path function is

$$ L_\bullet(z,\theta,\phi) = {}_s\epsilon(z)\sigma(z,\beta_s) + \int_{4\pi} L(z,\theta',\phi')\sigma(z,\beta')d\Omega \tag{2} $$

where $\sigma(z,\beta)$ is the directional volume scattering function at a scattering angle β, and ${}_s\epsilon(z)$ is the solar scalar irradiance at altitude z.

The development from these fundamentals to expressions for the inherent and apparent spectral contrasts C_r and C_o of a target t against its background b is straight forward and results in the directional contrast transmittance along the path r as given by

$$ C_r(z,\theta,\phi)/C_o(z,\theta,\phi) = T_r(z,\theta,\phi){}_bL_o(z,\theta,\phi)/{}_bL_r(z,\theta,\phi) \tag{3} $$

As emphasized by Duntley, et al. (1957), Eq. (3) does not involve restrictive assumptions and defines the law of contrast reduction in its most general form. It should be noted that Eq. (3) is expressed in terms of inherent and apparent background radiances ${}_bL_o$ and ${}_bL_r$, and is thus independent of target characteristics.

5. MODEL FOR ESTIMATING SLANT-PATH CONTRAST TRANSMITTANCE

The inherent variability of atmospheric structure and behavior and the complexities of radiative transfer processes require effective simplifying assumptions in order that estimates of contrast transmittance along any slant path in the atmosphere can be made rapidly and consistently. In pursuit of this objective, a series of modelling approximations relating optical properties to meteorological variables were derived from the broad experimental data base generated by airborne and surface measurement program. These relationships were combined with available analytic approximations for radiative transfer calculations to develop an operational technique for the estimation of directional path radiance and contrast transmittance. A detailed description of the model development and validation are presented in a report now being prepared for publication. A brief summary of the technique and several examples of model performance are given in the following paragraphs.

The calculation of the slant-path contrast transmittance with Eq. (3) requires consistent estimates of interrelated physical parameters. These include: (a) the vertical profile of total volume scattering coefficient, $s(z)$, (b) the vertical profile of the phase function for single scattering, $[\sigma(z,\beta)/s(z)] = P(z,\beta)$, and (c) vertical profile of single scattering albedo, $\omega(z) = s(z)/\alpha(z)$, where $\alpha(z)$ is the total volume attenuation coefficient. It should be emphasized that the contrast transmittance along any slant path depends primarily upon the extinction coefficient distribution both along the path and in the surrounding atmosphere. Accordingly, an attempt was made to condition the approximation procedures for all parameters on the existing capability to model and predict the extinction coefficient structure and behavior from conventional meteorological measurements and observations.

5.1. Estimates of the scattering ratio profile

For profile modelling purposes, it is important to consider a conservative measure of scattering coefficient that in the absence of local sources or sinks does not change appreciably following the air motion. The photopic scattering mixing ratio, $Q(z)$, is such a parameter. As the vertical mixing within an identifiable atmospheric layer becomes more complete, $Q(z)$ becomes more constant with height within the layer. The optical scattering ratio is defined $Q(z) = s(z)/s_R(z)$, where $s_R(z)$ is the total volume coefficient for Rayleigh scattering at altitude z.

Profiles of $Q(z)$ derived from the extensive series of airborne optical measurements made by the Visibility Laboratory, reveal large variability depending upon the aerosol source strength and the nature of the convective and turbulent mixing processes. The problem is to model the essential characteristics of the $Q(z)$ profiles in a way that recognizes the operational observing and forecasting limitations yet takes maximum advantage of existing capabilities. A prominent feature of the daytime aircraft soundings of optical scattering is the marked tendency for $Q(z)$ to remain essentially constant with height in the troposphere above the haze layer and also within the low-level haze layer. The difference in $Q(z)$ between adjacent tropospheric layers is typically much larger than the vertical variability within each layer. It should be emphasized that the assumption of constant scattering ratio with height does not hold well for ground-based stable layers with little vertical mixing such as those associated with the nocturnal formation of fog. The computer code developed for this modelling effort has provision for up to 20 atmospheric layers for use in complex situations when detailed information about the extinction coefficient profile is available. However, for application to problems of contrast transmittance in hazy atmospheres in the daytime following the dispersion of any surface inversion existing at sunrise, it is reasonable to employ a model consisting of a stratospheric layer and two or three tropospheric layers of constant optical scattering ratio. Thus, the forecasting problem is reduced to the prediction of the altitude limits of the atmospheric layers and the scattering ratio within each layer.

5.2. Specification of the phase function for single scattering

The asymmetry of the phase function for single particle scattering depends in a complex way on the size distribution and refractive index of the aerosols present in the atmosphere and the wavelength of incident light. The prominent feature of aerosol scattering is that as the particle size increases with respect to the wavelength, the amount of energy scattered in directions close to that of the incident radiation increases markedly causing larger asymmetry in the phase function. Since the total volume scattering coefficient varies approximately as the square or cube of the particle radius depending upon the size parameter, we might expect that the scattering coefficient or scattering ratio, $Q(z)$, might provide, through analytic representation, a good first approximation for the single scattering phase function. Experimental evidence shows this to be true.

The approach used herein for model development was first to represent the single scattering phase function for Mie scattering $P_M(z,\beta)$ by two term Henyey-Greenstein functions (Kattawar, 1975) as follows,

$$P_M(\beta,g_1,g_2,c) = c\,P_1(\beta,g_1) + (1-c)P_2(\beta,g_2)\,, \tag{4}$$

and

$$P(\beta,g) = (1-g^2)/\,[\,4\pi(1-2g\cos\beta+g^2)^{3/2}\,]\,, \tag{5}$$

where the asymmetry factor, g, is given by

$$g = \frac{1}{2}\int_0^{\pi} P(\beta)\cos\beta\sin\beta d\beta\,. \tag{6}$$

The phase function for single scattering has the normalized form,

$$\int_{4\pi} P(z,\theta,\phi)d\Omega = 1\,. \tag{7}$$

In turn, each of the Henyey-Greenstein parameters, $g_1(z)$, $g_2(z)$ and $c(z)$ were approximated as continuous functions of the Mie scattering ratio, $Q(z)-1$. The relationships between the phase function for combined aerosol and molecular scattering and the scattering ratio are bounded by the Rayleigh phase function $(Q=1, g=0)$ for a clear atmosphere and by a phase function representative of dense clouds or fog for very large $Q(z)$. Combined analysis of the asymmetry parameters (g_1,g_2,c) as derived from a least-squares fit of the Henyey-Greenstein functions to the average phase functions measured by Barteneva (1960) and to the phase functions derived from Mie calculations using typical aerosol distributions in haze and fog led to a consistent set of empirical equations expressing the asymmetry parameters as a function of the logarithm of the Mie scattering ratio, $(Q-1)$.

Independent evidence of the general applicability of the model estimates of $P(\beta)$ with respect to wavelength and altitude is given by a comparative study of directional scattering functions that were measured by the Visibility Laboratory airborne nephelometer and the Barteneva (1960) phase function measurements (see Section 3 and Fig. 6). In addition to the measurement of total volume scattering coefficient, the integrating nephelometer measured, separately, the directional scattering function at nominal scattering angles of 30^o and 150^o in four wavelength bands centered near 475, 550, 660, and 750 nm. The analysis by Johnson, et al. (1979) of the airborne data gathered by the Visibility Laboratory in Europe and the United States over all seasons indicates that the derived relationship between the phase functions scattering ratio holds well over all visible wavelengths and over all altitudes up to the highest levels sampled by the instrumented aircraft (usually near 6 km). Figures 8 and 9 show a comparison of phase functions as calculated from the model, calculated from Mie theory, and measured by Barteneva.

To the extent that more accuracy is desired and more complete information is available to define $P(z,\beta)$, the overall computer code for calculating path radiance and contrast transmittance was made general in that it will accept as input for each atmospheric layer any specified $P(z,\beta)$. However, in the absence of information other than an estimate of $Q(z)$, calculation of $P(z,\beta)$ from the system of model equations is recommended for haze only atmospheres. Important details typical of phase functions for fog conditions such as the prominent minimum near $\beta = 100°$ and the secondary maximum near 140^o (see Fig. 9) are smoothed out by the representation with Henyey-Greenstein functions. It should be emphasized that important additional evidence of the applicability of the model for estimating $P(z)$ from $Q(z)$ will be obtained as we employ the technique more extensively for the specification of the sky and terrain radiances as measured in various deployments of the instrumented aircraft. Sample comparisons of measured and computed radiances are given in the following section.

5.3. Calculation of the path radiance component due to scattering of diffuse irradiance

As given by the first term on the right hand side of Eq. (2), the component of the directional path function produced by the scattering of direct solar irradiance incident on the path is calculated from estimates of the single scattering phase function determined by the technique described in the previous paragraphs. The second term on the right hand side of Eq. (2) is the component of path function resulting from the scattering of diffuse irradiance reaching the path from the surrounding sky and terrain. As in the case of the direct solar component, the directional dependence of the diffuse background contribution to the path radiance must be considered. Precise numerical

calculation of the radiance distribution resulting from the complex multiple scattering processes requires large amounts of computer time. For this reason, great emphasis has been placed upon the development of rapid approximate methods for radiation transfer calculations (Meador and Weaver, 1980). The appropriate choice of computational method from among the variety of available methods depends upon the results desired for the application at hand.

While it is important to retain complete directionality for calculation of the path radiance component due to single scattering of direct solar irradiance, approximate two stream methods often can be used effectively for fast calculation of the component due to scattering of diffuse irradiance provided that the asymmetric influence of the prominent forward scatter peak is managed adequately. The delta-Eddington approximation introduced by Joseph, Wiscombe and Weinman (1976) satisfies the requirement. It differs from the standard Eddington approximation, which assumes a simple cosine dependence of the single scattering phase function, in that it approximates the phase function by a truncated forward scatter peak and a two-term phase function expansion,

$$P_d(\beta) = 2f'\,\delta(1-\cos\beta) + (1-f')(1+3g'\cos\beta)\,, \tag{8}$$

where f' is the fractional scattering represented by the forward peak and g' is the asymmetry factor of the truncated phase function. In effect, the delta-Eddington approximation transforms most of the scattered radiation in the solar aureole into the direct solar flux component, and assumes that

$$f'(z) = g^2(z)\,. \tag{9}$$

As an integral part of the technique for estimating directional contrast transmittance, the approximate diffuse radiance, $[L_D(z) + L_{D'}(z)\cos\theta]$, calculated by the Eddington computer code (Shettle and Weinman, 1979), as modified by the delta-Eddington approximation, is used directly to obtain the second term on the right hand side of Eq. (2); so that this component of the path function generated by the scattering of diffuse irradiance is given by

$$\int_{4\pi} L(z,\theta',\phi')\,\sigma(z,\beta')\,d\Omega = L_D(z) + \frac{2}{3}\,L_{D'}(z)\cos\theta\,. \tag{10}$$

5.4. Calculation of directional path radiance and contrast transmittance

With the procedures for estimating the direct and diffuse components described above, the directional path radiance L_r^* can be calculated from Eqs. (2) and (3) by finite summation over successive atmospheric layers using the trapezoidal rule. The computer code for calculation of directional path radiance and contrast transmittance along any slant path in accordance with Eqs. (1) through (8) requires the following input:

1) a representative wavelength λ that is commensurate with the spectral response of the sensor in μm
2) the solar irradiance $E_s(\infty)$ at the upper limit of the atmosphere in $w/m^2\mu m$ corresponding to spectral response of the sensor
3) the number of atmospheric layers n and the altitude z_n of the base of each layer in km
4) the average optical scattering ratio $Q(z)$ for each atmospheric layer
5) the average single scattering albedo $\omega(z)$ for each atmospheric layer
6) the average surface reflectance $R(\theta,\phi)$ and the reflectance of the immediate background of the viewed object if significantly different than the albedo of the general background
7) the object and observer altitudes in km and the viewing angle with respect to the sun, β, and zenith, θ, in degrees
8) the solar zenith angle θ_s in degrees.

6. RESULTS OF MODEL CALCULATIONS

Model calculations based upon the extensive data gathered by the airborne measurement program make possible a close analysis of the dependence of optical properties on meteorological conditions. Comparative analyses of observed data with the model calculations are being used to improve techniques for the prediction of image transmission properties from conventional meteorological observations. Some

trial model calculations are illustrated in the following paragraphs.

Comparisons of the sky and terrain radiance distribution measured by the scanning radiometers and the model calculations of the radiance distribution from the observed input parameters are shown in Figs. 10 and 11 for the flight made on 15 August 1978 in northwestern Germany near Meppen. A 3-layer atmosphere was assumed for model calculations with the top of the haze layer at 1.3 km (see scattering coefficient profile in Fig. 5) and a tropopause height of 10 km. The observed features of the radiance distribution are typical of rural clear sky conditions observed in western Europe in the summer months. At the observation altitude deep within the haze layer at 200m, the sky radiance in the upsun direction, $\phi = 0°$, is substantially larger than the view angle away from the sun, $\phi = 180°$. However, the disparity in sky radiances in the upsun and downsun directions is much smaller looking upward from an altitude well above the haze layer near 6 km. The rather large fluctuations in measured radiance looking downward from the low altitude of 200m are caused by differences in the reflectivity of various terrain pattern features such as the green and brown fields and small wooded areas.

For the same experimental flight, Fig. 12 shows the contrast transmittance distribution for downward view angles from an observation level of 6 km and target altitude of 0.2 km that were calculated from the radiance distribution given by both the aircraft measurements and the model calculations. Looking overhead, Fig. 13 shows the apparent contrast as a function of zenith angle for an object at 20 km viewed from 0.2 km as calculated from the observed and model sky radiance distributions.

The model calculations can be used to assess quantitatively the changes in contrast transmittance associated with incremental changes in the individual environmental factors governing image transmission in the atmosphere. For purposes of illustration, the reference atmosphere as described in Table 2 was derived from the measurements made on 15 August 1978 near Meppen, Germany (see Fig. 5). As discussed above, the meteorological conditions observed on this flight are representative of clear sky conditions for this geographical area and time of the year. An optical scattering ratio of 16 for the haze layer converts to a horizontal visual range of about 16 km at the surface assuming an inherent target contrast of -1, no absorption and an apparent contrast threshold for detection of 5 percent. The single scattering albedo of 0.83 assumed for the haze layer is commensurate with measurements in rural areas in the United States by Weiss, et al. (1980).

For a specified azimuth angle, the slant range between the sensor and target altitudes where the apparent contrast of the target and background reduces to a fixed threshold value can be determined from systematic model calculations for successive zenith view angles. Calculation of the slant range corresponding to 5 percent apparent contrast for the reference atmosphere specified in Table 2 and for a series of individual incremental changes in various atmospheric variables are illustrated in Fig. 14. It should be emphasized that the indicated changes in slant range as a function of changes in the input variables are specific only for the variations about the given set of conditions, i.e. observation level at 20 km, target at surface, target reflectivity of 50 percent, azimuth view angle of zero with respect to the sun, and atmospheric structure as given by the reference atmosphere. However, the results illustrated here do provide insight into the relative impact of the parameter changes on contrast transmittance. Using approximate interpolation methods under the same prescribed conditions, we have calculated the changes in individual parameters which produce a family of equivalent effects. Thus, Table 3 illustrates those changes in conditions, any one of which will result in a corresponding 20% decrease in apparent contrast.

7. SUMMARY

The computer model developed during the course of the experimental optical measurement and analysis program can provide relatively fast and consistent estimates of optical atmospheric properties over any slant path as a function of wavelength in the visible spectrum. To the extent that a climatological data base of conventional meteorological observations exists, the technique in its present form can be used to estimate readily the frequency distributions of such quantities as spectral contrast transmittance as a function of location and season.

Refinements in the model are being made as validation tests and experiments continue. Early results indicate that further parameterization of selected components of the model can be made which will improve computational efficiency and at the same time retain the capability to take advantage of any and all relevant observational and forecast information. A realistic goal is to employ the computer model as part of a data acquisition and microprocessing system for real time estimates of image transmission properties. Future experiments are planned to examine the tradeoffs between the type, accuracy, frequency and density of optical/meteorological observations and the

8. ACKNOWLEDGEMENTS

The studies conducted prior to and during the preparation of this paper have involved the talents and skills of many persons associated with both the Air Force Geophysics Laboratory and the University of California, Visibility Laboratory. The authors gratefully acknowledge these contributions, and in particular would like to thank Dr. Robert Fenn and Mr. Eric Shettle of the Geophysics Laboratory and Ms. Jacqueline I. Gordon of the Visibility Laboratory for many constructive discussions, comments and suggestions.

This effort has been supported by the Air Force Geophysics Laboratory under Contract No. F19628-78-C-0200.

9. REFERENCES

Barteneva, O. D. (1960), "Scattering Functions of Light in the Atmospheric Boundary Layer," Bull. Acad. Sci. U.S.S.R., Geophysics Series, 1237-1244.

Duntley, S. Q., A. R. Boileau, and R. W. Preisendorfer (1957), "Image Transmission by the Troposphere I", J. Opt. Soc. Amer., 47, 499-506.

Duntley, S. Q., R. W. Johnson, J. I. Gordon, and A. R. Boileau (1970), "Airborne Measurements of Optical Atmospheric Properties at Night," University of California, San Diego, Scripps Institution of Oceanography, Visibility Laboratory, SIO Ref. 70-7, AFCRL-70-0137. NTIS, Ad 870 734.

Duntley, S. Q., R. W. Johnson, and J. I. Gordon (1977), "Airborne Measurements of Atmospheric Volume Scattering Coefficients in Northern Europe, Spring 1976," University of California, San Diego, Scripps Institution of Oceanography, Visibility Laboratory, SIO Ref. 77-8, AFGL-TR-77-0078. NTIS, ADA 046 290.

Duntley, S. Q., R. W. Johnson, and J. I. Gordon (1978a), "Airborne Measurements of Optical Atmospheric Properties, Summary and Review III," University of California, San Diego, Scripps Institution of Oceanography, Visibility Laboratory, SIO Ref. 79-5, AFGL-TR-78-0286. NTIS, ADA 073 121.

Duntley, S. Q., R. W. Johnson, and J. I. Gordon (1978b), "Airborne Measurements of Atmospheric Volume Scattering Coefficients in Northern Europe, Fall 1976," University of California, San Diego, Scripps Institution of Oceanography, Visibility Laboratory, SIO Ref. 78-3, AFGL-TR-77-0239. NTIS, ADA 057 144.

Fenn, R. W. (1978), "OPAQUE - A Measurement Program on Optical Atmospheric Properties in Europe, Vol. I. The NATO OPAQUE Program," Special Reports No. 211, AFGL-TR-78-0011.

Johnson, R. W. and J. I. Gordon (1980), "Airborne Measurements of Atmospheric Volume Scattering Coefficients in Northern Europe, Summer 1978," University of California, San Diego, Scripps Institution of Oceanography, Visibility Laboratory, SIO Ref. 80-20, AFGL-TR-80-0207.

Johnson, R. W., W. S. Hering, J. I. Gordon, B. W. Fitch and J. E. Shields (1979), "Preliminary Analysis and Modelling Based Upon Project OPAQUE Profile and Surface Data," University of California, San Diego, Scripps Institution of Oceanography, Visibility Laboratory, SIO Ref. 80-5, AFGL-TR-79-0285. NTIS, ADB 052 172L.

Johnson, R. W. (1981), "Daytime Visibility and Nephelometer Measurements Related to its Determination," Paper presented at Environmental Protection Agency Symposium on Plumes and Visibility, Grand Canyon, Arizona, Nov. 1980. Accepted for publication, ATMOSPHERIC ENVIRONMENT, Dec. 1980.

Joseph, J. H., W. J. Wiscombe, and J. A. Weinman (1976), "The delta-Eddington Approximation for Radiative Flux Transfer", Atmos. Sci., 33, 2452-2459.

Kattawar, G. W. (1975), "A Three-Parameter Analytic Phase Function for Multiple Scattering Calculations", J. Quant. Spectrosc. Radiant. Transfer, 15, 839-849.

Meador, W. E., and W. R. Weaver (1980), "Two Stream Approximations to Radiative Transfer in Planetary Atmospheres: A Unified Description of Existing Methods and a New Improvement", J. Atmos. Sci., 37, 630-643.

Shettle, E. P., and J. A. Weinman (1970), "The Transfer of Solar Irradiance Through Inhomogeneous Turbid Atmospheres Evaluated by Eddington's Approximation", J. Atmos. Sci., 27, 1048-1055.

Weiss, R. E., R. J. Chankan, A. P. Waggoner, N. Sadler, and J. Ognen (1980), "An Assessment of Light Absorption by Aerosol Particles in Urban, Rural and Remote Troposphere and Stratospheric Air", 1980 International Radiation Symposium Extended Abstracts, International Association of Meteorology and Atmospheric Physics, IUGG, 178-180.

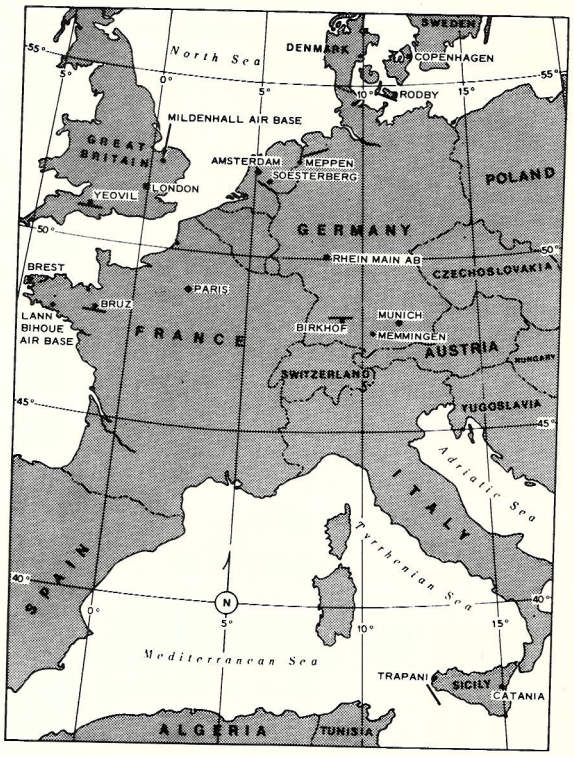

Fig. 2. Typical OPAQUE Flight Tracks.

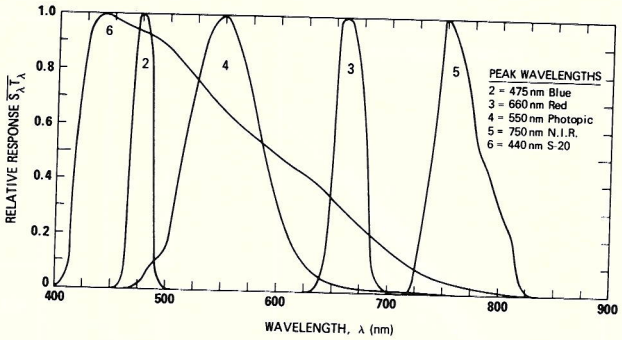

Fig. 1. Standard Spectral Responses.

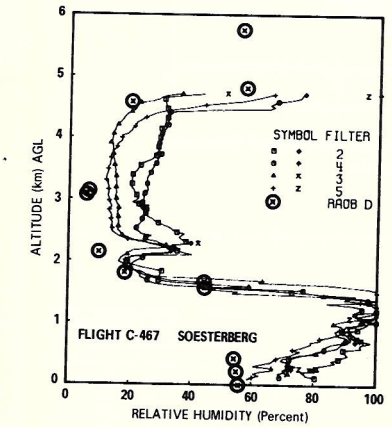

Fig. 4. Relative Humidity Profiles, Flight C-467.

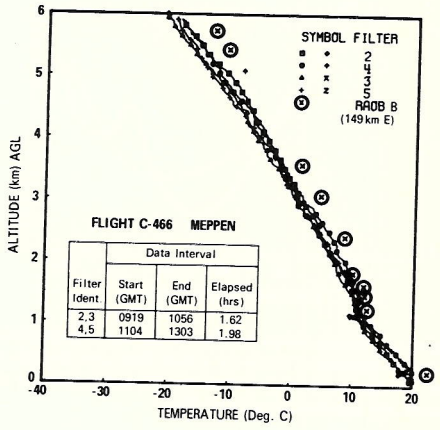

Filter Ident	Data Interval Start (GMT)	End (GMT)	Elapsed (hrs)
2,3	0919	1056	1.62
4,5	1104	1303	1.98

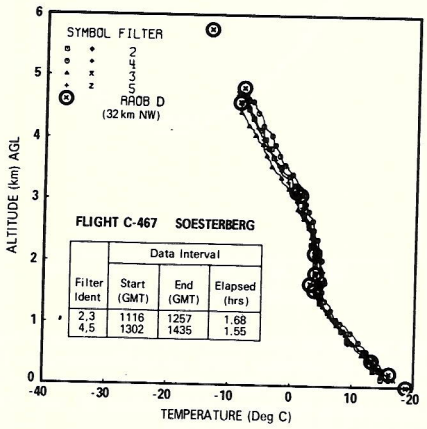

Filter Ident	Data Interval Start (GMT)	End (GMT)	Elapsed (hrs)
2,3	1116	1257	1.68
4,5	1302	1435	1.55

Fig. 3. Temperature Profiles, Flights C-466 & C-467.

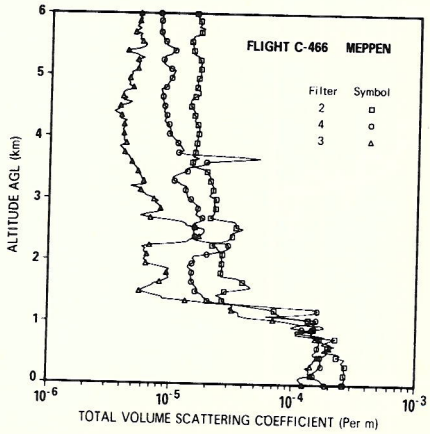

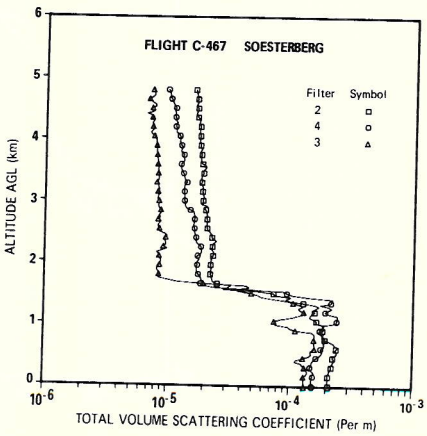

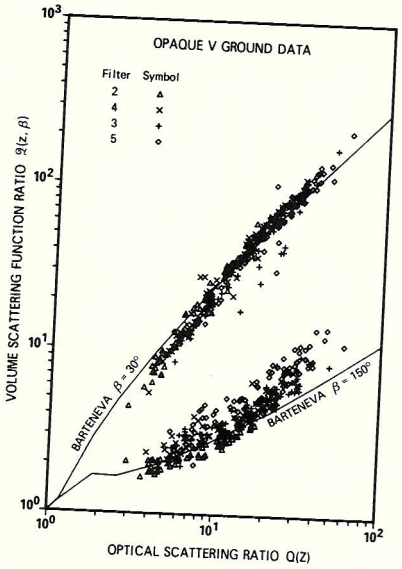

Fig. 6. Multi-Spectral Directional Scattering Measurements.

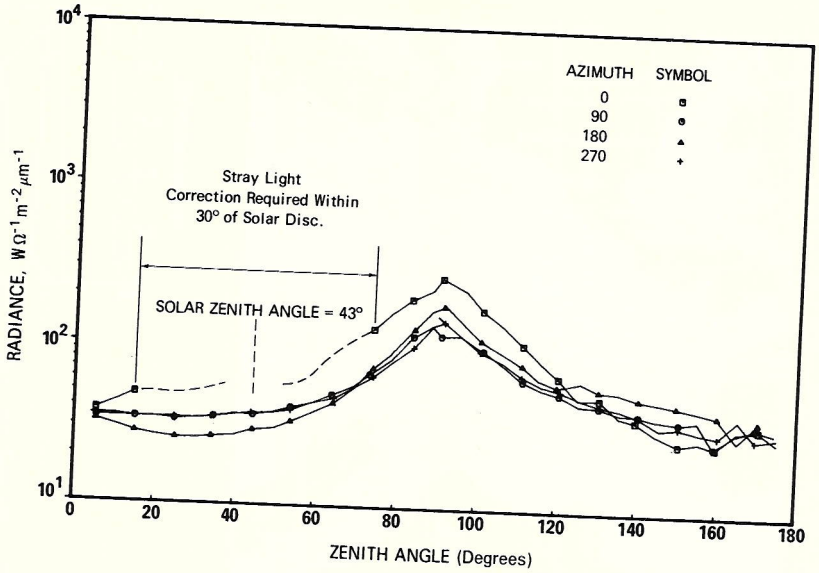

Fig. 7. Measured Sky and Terrain Radiance Distributions for Flight C-466, filter 2, 2953m AGL.

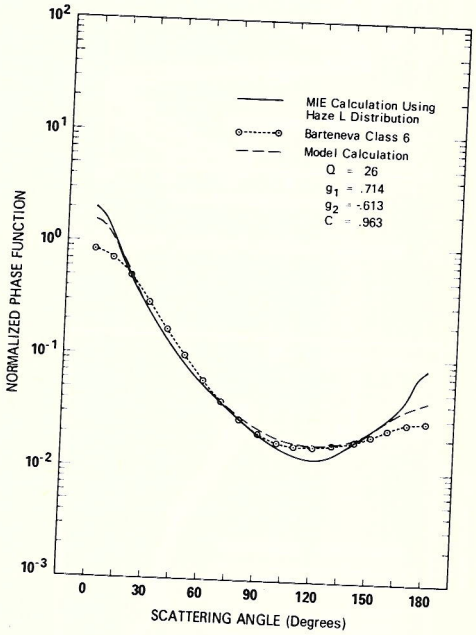

Fig. 8. Single scattering phase functions (a) calculated from Mie theory by Kattawar (1975) using Diermendjian (1969) Haze L distribution with a refractive index of 1.55 - 0.0i; (b) observed by Barteneva (1960) (class 6); and (c) calculated for scattering ratio of 26.

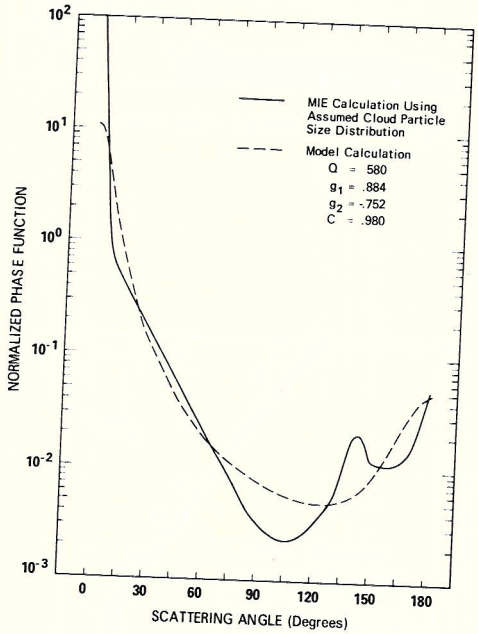

Fig. 9. Single scattering phase functions (a) calculated from Mie theory by Kattawar (1975) for cloud drop distribution $n = kr^6e^{-1.5r}$ and refractive index of 1.33 - 0.0i, and (b) calculated for scattering ratio of 580.

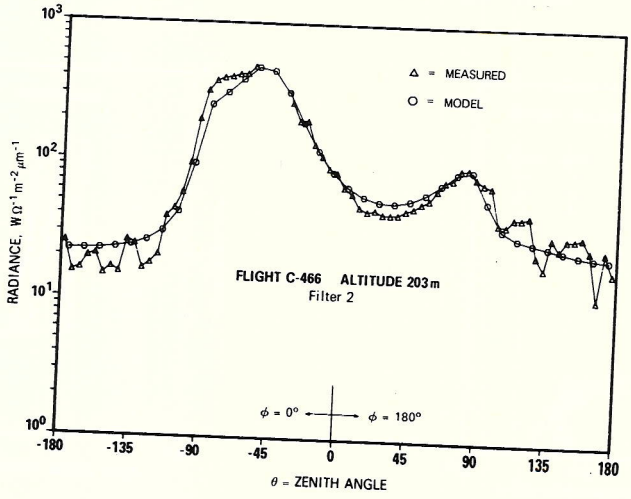

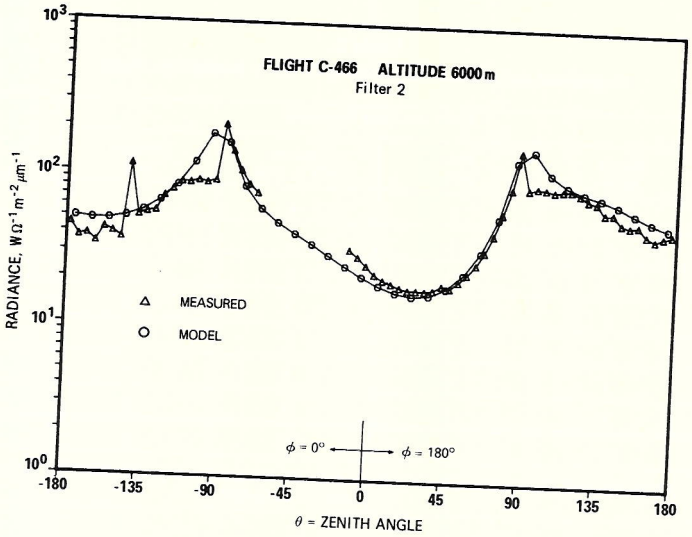

Fig. 11. Comparison of measured and calculated sky and terrain radiance distributions at 6000 m.

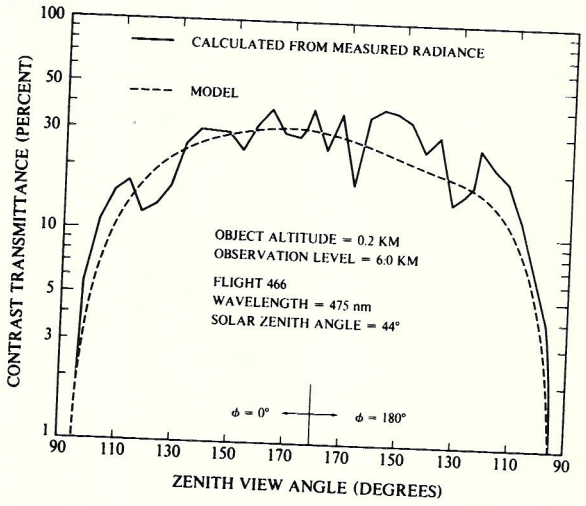

Fig. 12. Comparison of contrast transmittance distributions calculated from measured and observed sky and terrain radiance distributions.

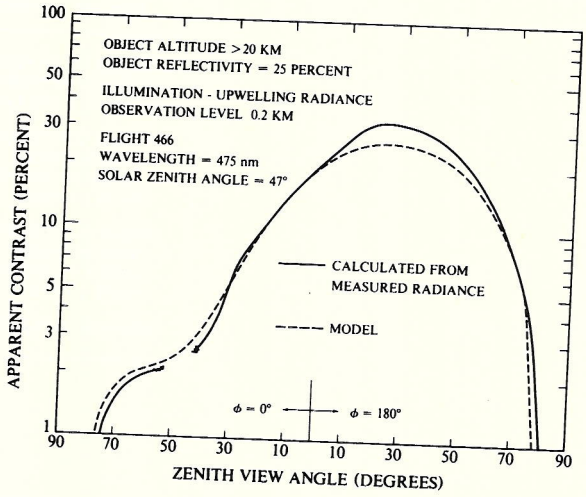

Fig. 13. Comparison of apparent contrast distributions calculated from measured and model sky radiance distributions.

OBJECT AT SURFACE INHERENT CONTRAST = 50%
OBSERVATION LEVEL = 20 KM AZIMUTH VIEW ANGLE = 0°
WAVELENGTH = 550 nm (PHOTOPIC)

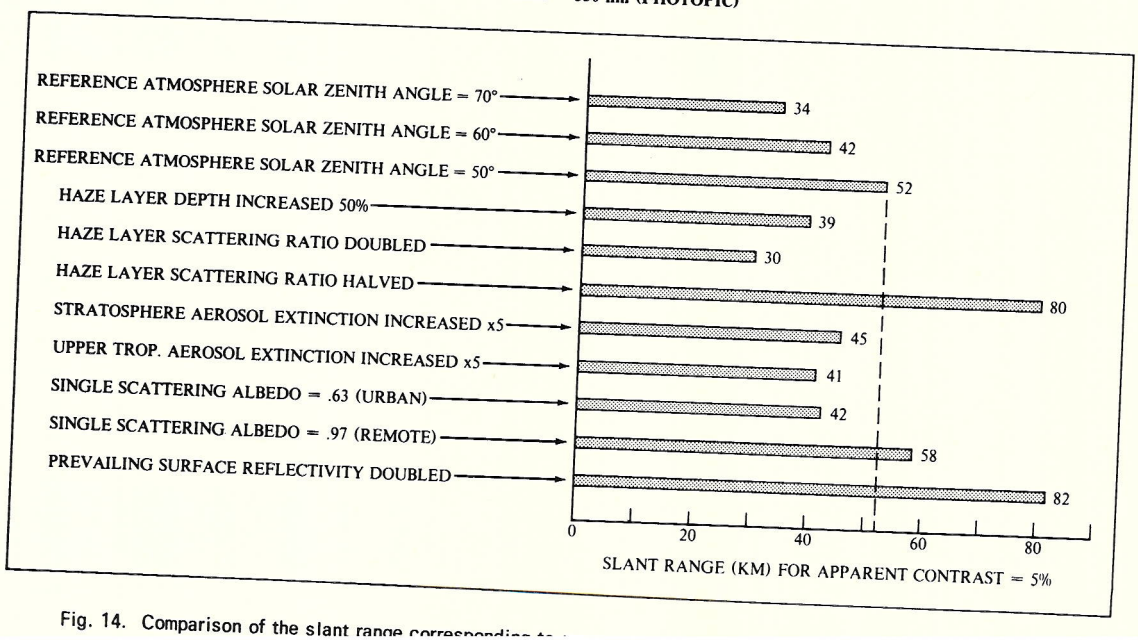

Fig. 14. Comparison of the slant range corresponding to

Table 1.

Geographical and Seasonal Distribution of OPAQUE Related Data Flights

Flight Location (Fig. 1)	Attempted Data Sequences				Totals
	Spring 1976	Fall 1976	Summer 1977 & 1978	Winter 1978	
Sicily	0	0	4	5	9
France	0	5	3	0	8
So. Germany	0	0	5	8	13
No. Germany	5	4	9	3	21
Netherlands	1	0	3	2	6
England	5	0	3	7	15
Denmark	2	4	6	2	14
Totals	13	13	33	27	86
Data Reports	AFGL-TR-77-0078	AFGL-TR-77-0239	AFGL-TR-78-0168 AFGL-TR-80-0207	AFGL-TR-79-0159	AFGL-TR-79-0285

Table 2.

Reference Atmosphere (Photopic, $\lambda = 550m$)

NUMBER OF LAYERS	3
ALTITUDE OF TROPOPAUSE	10 km
DEPTH OF HAZE LAYER	1.3 km
OPTICAL SCATTERING RATIO	
STRATOSPHERE	1.3
UPPER TROPOSPHERE	1.3
HAZE LAYER	16.0
SINGLE SCATTERING ALBEDO	
STRATOSPHERE	0.99
UPPER TROPOSPHERE	0.97
HAZE LAYER	0.83
SURFACE REFLECTANCE	0.07

Table 3.

Parametric Changes Inducing 20% Decrease in Apparent Contrast

Item	Parameter	Change	Amount
a.	Haze layer depth, Z	increase	30%
b.	Haze layer scattering ratio, $Q(z)$	increase	25%
c.	Haze layer single scattering albedo, $w(z)$	decreased	24%
d.	Mid-Troposphere Aerosol Scattering Coeff. $s(z)$	increase	factor of 3
e.	Stratosphere Aerosol Scattering Coeff. $s(z)$	increase	factor of 5.7